Understanding the formation of self-organized micro/nanostructures on metal surfaces from femtosecond laser ablation using stop-motion SEM Imaging

Craig A. Zuhlke*[a], Troy P. Anderson[a], Dennis R. Alexander[a]
[a]Department of Electrical Engineering, University of Nebraska-Lincoln, 844 N 16th St, Lincoln, NE USA 68588

ABSTRACT

There are a growing number of unique self-organized micro/nanostructures created using femtosecond laser surface processing that have been demonstrated. Although researchers have provided insight into the formation processes for distinctive morphologies on specific materials, there is a need for a broader understanding of the physics behind the formation of a wide range of morphologies and what parameters affect their formation. In this work, the formation processes for mound structures on 316 stainless steel (SS) with growth above the original sample surface are studied. The formation process for the structures on 316 SS is compared to similar structures formed on nickel using the same technique. The structures are formed using 800 nm, 50 fs laser pulses, and are self-organized, meaning the structure dimensions are much smaller than the spot size of the pulses used to create them. The formation dynamics were studied using a stop-motion scanning electron microscope (SEM) technique, where the same location of an irradiated sample was imaged in the SEM at various pulse counts. The result is a series of images showing the developmental progress with increasing pulse counts. The structures form through a combination of fluid flow of the surface melt that results after irradiation, preferential ablation of the center of the pits between structures, and material/nanoparticle redeposition.

Keywords: Femtosecond laser; ultrashort laser; laser microstructuring, light-matter interactions

1. INTRODUCTION

Femtosecond lasers are developing into a common tool for producing micro/nanostructured surfaces on a wide range of materials. Examples of self-organized surface structures that have been demonstrated using femtosecond laser surface processing (FLSP) include pillars[1-4], cones[5-7], spikes[3,8-10], mounds[11], and pyramids[12,13]. These structures have been shown to have their peaks either above or below the original surface depending on the parameters used. A key characteristic of the type of structure discussed here is that they are self-organized, meaning their dimensions are much smaller than the spot size of the focused pulses used to produce them.

Understanding the full formation dynamics for surface structures formed using FLSP has proven to be a complicated and an unfinished task. In order to aid in the understanding of the formation processes for these self-organized structures our group has developed a novel technique to visualize the step-by-step growth of self-organizing microstructures using a scanning electron microscope (SEM) alongside the FLSP system. Most FLSP that leads to self-organized micro/nanostructures is completed at a low repetition rate (1 – 10 kHz). At these low repetition rates, the material reaches steady-state conditions between each ablation pulse. Due to the steady-state and permanent nature of the surface between ablation pulses, it does not matter how much time is permitted between individual pulses. As a result there is time to capture high magnification images of the material between the ablation pulses. Images can be taken between pulses over the pulse/image count covering the full development of the structure. Each individual image can then be combined into a sequence forming a video. The resulting high magnification video can be used to document and study formation of the micro/nanostructure features on a surface. These high-resolution videos can then be used to document the full developmental surface changes and in particular the formation of micro and nanostructures[11,12].

We have previously utilized this technique to study the formation of three unique surface structures on nickel: above surface growth mounds (ASG-mounds), below surface growth mounds (BSG-mounds) and nanoparticle covered pyramids (NC-pyramids)[11-13]. ASG-mounds and BSG-mounds are similar in appearance with a height to width aspect

*czuhlke@unl.edu

Laser-based Micro- and Nanoprocessing VIII, edited by Udo Klotzbach, Kunihiko Washio, Craig B. Arnold,
Proc. of SPIE Vol. 8968, 89680C · © 2014 SPIE · CCC code: 0277-786X/14/$18 · doi: 10.1117/12.2040348

ratio of at least 2:1, and widths in the range of 5-10 μm. The fundamental difference in morphology between the two structures is that ASG-mounds have peaks that extend above the original sample surface while BSG-mounds have peaks below the original sample surface[11]. In this paper we extend the stop-motion SEM imaging technique to 316 stainless steel (SS), and show that the formation process for ASG-mounds is different on 316 SS than it is on nickel, particularly in the formation of precursor sites.

2. EXPERIMENT

The laser used for this research was a Spitfire, Ti:Sapphire laser system from Spectra Physics capable of producing 1 mJ, 50 fs pulses at a 1 kHz repetition rate. Using a fast shutter, the repetition rate was controlled down to single pulses. The laser pulses were monitored using a Frequency Resolved Optical Gating (FROG) instrument from Positive Light (Model 8-02). The growth of the ASG-mounds on 316 SS was documented using the stop-motion SEM technique described in our previous publication[11]. With this technique high magnification SEM images are taken of the sample in between the incidence of single pulses on the sample. With each pulse the sample was aligned to the same location relative to the focal volume. The result of this technique is a series of high magnification SEM images of the same location on the sample with increased pulse count that were then combined into a video format. We demonstrated in our previous publications that the fluence is a critical parameter that determines the type of structure that develops during the ablation process[11,12]. In order to get a constant fluence over a large region, a square flat top beam profile was utilized. A specialized refractive beam shaper from Eksma Optics (GTH-4-2.2FA) was used to convert the Gaussian pulses out of the laser to a square flat top profile at the system focus. The experimental setup and beam profile can be seen in our previous publication[11]. On 316 SS the ASG-mounds develop over a range of about 200 pulses. SEM images were taken between each pulse for the first 20 pulses and then every 5 pulses after that, up to a total of 200 pulses. The square spot size used for this research was about 210 μm x 210 μm and the laser fluence was 1.3 J/cm^2. For comparison purposes, SEM images are also included of ASG-mounds on Nickel. For the results on Nickel, a 150 μm x 150 μm square spot size was used with a pulse fluence of 3.08 J/cm^2.

3. RESULTS AND DISCUSSION

As reported in our previous publications on nickel, the transition from BSG-mounds to ASG-mounds occurs at a fluence around 2 J/cm^2. However, on 316 SS the threshold fluence between the two classes of structures is much lower, and a fluence of 1.3 J/cm^2 is in the regime where ASG-mounds develop. This cutoff region is currently undocumented for 316 SS, however, the growth the mounds above the original surface after 200 ablation pulses can be seen in Fig. 1(a) and (b). The final morphology for the ASG-mounds on 316 SS (see Fig. 1(c)) is very similar in appearance to those formed on nickel (see Fig. 1(d)). However, there are differences in the formation process of the structures for the two materials.

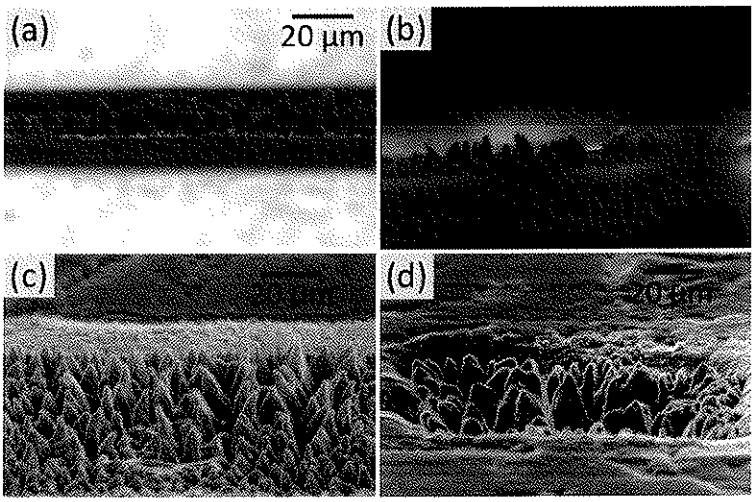

Figure 1. (top) SEM images of the resulting ASG-mounds after 200 pulses with the stop-motion SEM technique, viewed at a steep angle to show the growth of the structures above the original surface. (bottom) SEM images of ASG-mounds on (a) 316 SS formed using 200 pulses and (b) Nickel (200/201) formed using 180 pulses.

The material used for this research was unpolished 316 SS, which had an initially rough surface. The surface roughness with the initial grooves can be seen in Fig. 3(a), which is an SEM image after a single ablation pulse was incident on the surface. With the early pulses (>40 pulses) the rough surface began to smooth out eliminating the grooves in the unprocessed surface as seen in Fig. 3(b) and (c). This smoothing process does not play a role in the development of the ASG-mound structures. Through other research, not presented here, we have found that the ASG-mounds form on polished 316 SS without a noticeable difference in the final morphology compared to using the unpolished 316 SS.

In these early pulse counts, the formation of ASG-mounds is different on 316 SS than it is on Nickel. With ASG-mound formation on Nickel the surface is covered in random nanostructure as a result of the initial pulses. An example of this random nanostructure after 10 pulses can be seen in Fig. 2(a). The random nanostructure then leads to increased absorption of subsequent pulses and therefore a deeper surface melt. It is the formation of this random nanostructure and the resulting increased absorption that eventually results in the development of the micro-ripples followed by the precursor domes[11]. An example of these micro-ripples along with some of the precursor cones can be seen in Fig. 2(b). On 316 SS the random nanostructure never develops and instead the surface becomes smoother than its original state. It should be noted that upon close inspection some nanoparticles can be seen on the 316 SS sample. The larger of these nanoparticles can be as dots throughout the SEM images in Fig. 3.

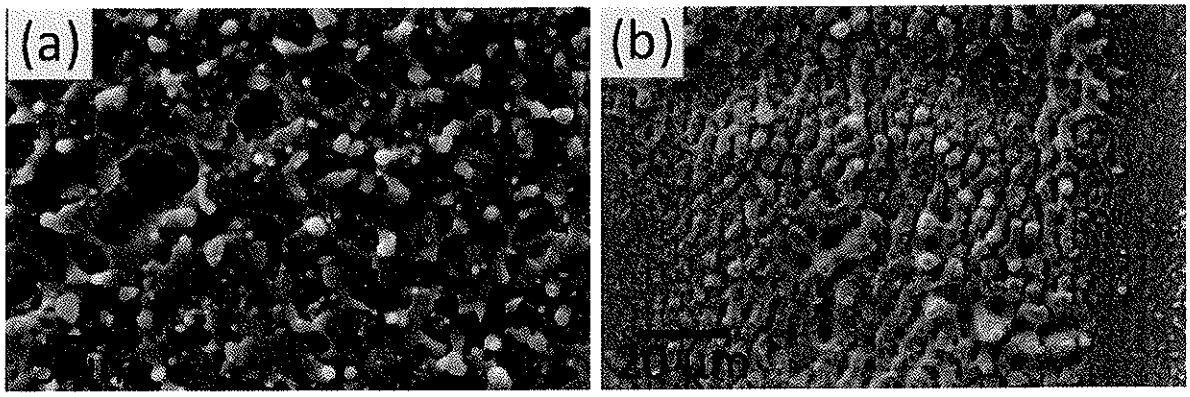

Figure 2. SEM images of ASG-mound development on Nickel formed at 3.08 J/cm^2 after (a) 10 pulses (b) 55 pulses.

The full development process for ASG-mounds on 316 SS can be seen in the series of images in Fig. 3 and Fig. 4, which are images of the sample location at different magnifications. The corresponding videos, Vid. 1 and Vid. 2, give a clear visualization of the development process. The development of ASG-mounds on 316 SS is summarized in two phases in the discussion that follows.

3.1 Phase I: Development of precursor pits and domes

In much of the work reported in the literature using FLSP, the formation of the microstructures includes the formation of laser induced periodic surface structures (LIPSS)[16-18] or micro-ripples[19-26]. In our previous publication on the formation of ASG- and BSG-mounds on nickel, we showed the mounds form at a fluence well above the regime for LIPSS formation and so the development is independent of LIPSS. The initial stages of formation on nickel does include the formation of micro-ripples, which are periodic ripples with a period between 2.5 – 5 μm[11]. With 316 SS, the ASG-mounds fully develop with no periodic structure formation. Instead, the precursors for ASG-mound growth on 316 SS are randomly oriented pits. Once a pit develops, it grows larger through a preferential ablation process, where reflections off the side walls focus light into the center causing the pit to grow larger at an accelerated rate. It is unclear what leads to the initial pit formation, but on the current sample many of the pits form in the grooves initially present on the sample. On a polished sample, the pits could develop from a localized decrease in ablation threshold, for instance from impurities in the surface, or from the inhomogeneous redeposition of material or nonuniform flow of the surface melt from early pulses. Once a pit develops, material flows from the bottom of the pit up the sides eventually forming a rim of material on the outer edge. This hydrodynamic process is likely a result of non-uniform heating of the pit. The glancing angle on the side of the pits results in low absorption and reflection of light into the center of the pit. The result is a hotter surface melt in the center than on the sides and a flow of the melt up the sides, similar to the process described for the growth of columns using nanosecond pulses[11,14,15]. With increased pulse count, more pits develop and the pits grow larger. Whenever two pits form close together the intersection of the rim from each pit leads to the formation of a dome.

It should be noted that even on nickel there are some ASG-mounds that form from precursor pits, similar to those described here, however, with Nickel the micro-ripples are always present in the early stages of development.

3.2 Phase II: Upward growth of ASG-mounds

Once the domes have formed the second phase of ASG-mound development begins. With increased pulse count the domes grow taller and develop into ASG-mounds. Once formed the ASG-mounds grow taller through two possible mechanisms similar to ASG-mound growth on Nickel: fluid flow of material from the bottom of the pits up the sides of the structures; or vapor liquid solid (VLS) growth[11]. The fluid flow process is a hydrodynamic process similar to the formation of the rims around the pits described in phase I. VLS growth is a process where ablation leads to the formation of a vapor cloud around the structure. Since the top of the structure is melted from the incident ablation pulse a reaction with the vapor cloud occurs at the peak, causing the structure to grow taller. The fluid flow aspect is clear from the videos, while the VLS is not as evident on 316 SS as it is on Nickel[11].

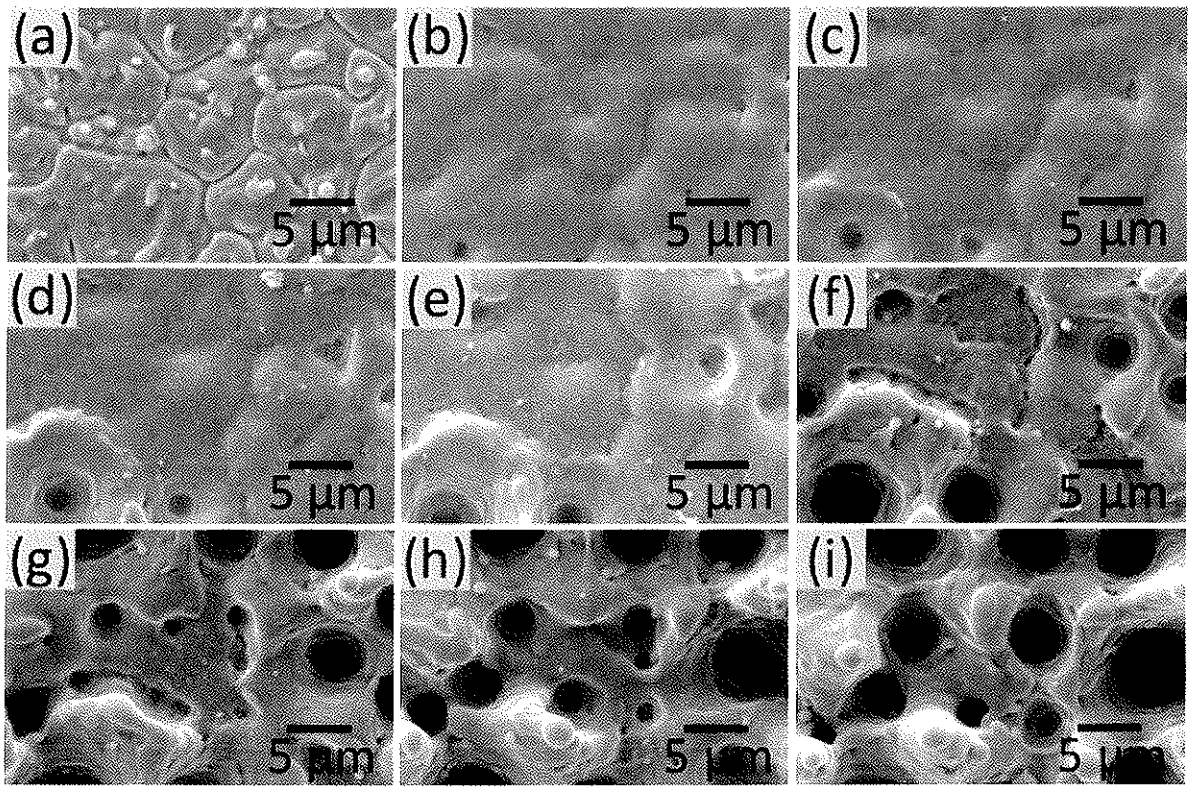

Figure 3. SEM image of stepped spike growth on SS316 using 1.3 J/cm2, after (a) 1, (b) 20, (c) 40, (d) 60, (e) 80, (f) 100, (g) 120, (h) 140, and (i) 160 pulses.

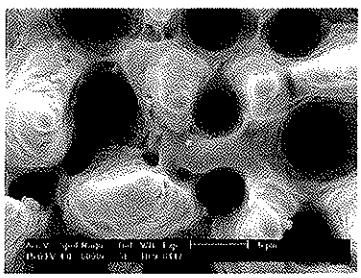

Video 1. File: video 1; Video of SEM images of spike growth on 316 SS with increased pulse count at 8000x magnification.
http://dx.doi.org/10.1117/12.2040348.1

Precursor pits continue to develop at various pulse counts. In these experiments the first pits showed up around 20 pulses. With increased pulse counts more pits develop increasing the density of the ASG- mound and covering more of the surface. The pit development throughout the pulse count range can be seen in the series of images in Fig. 4 and corresponding Vid. 2.

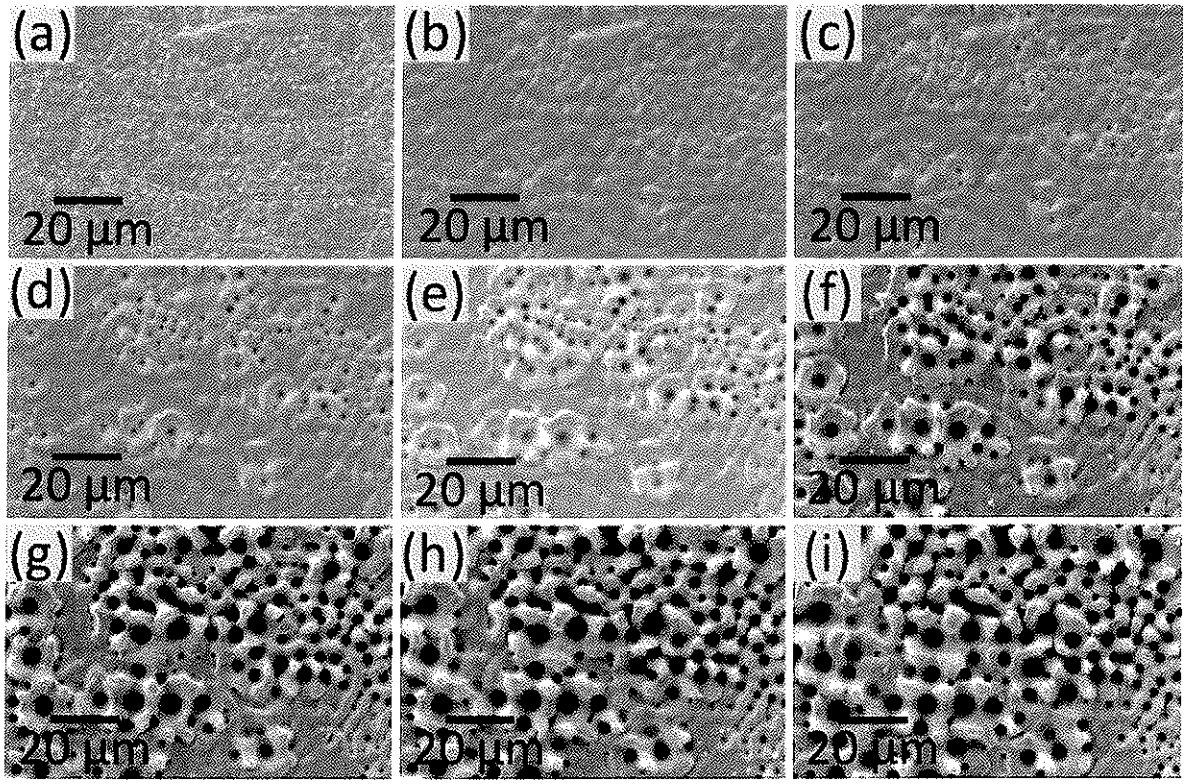

Figure 4. SEM image of stepped spike growth on SS316 using 1.3 J/cm2, after (a) 1, (b) 20, (c) 40, (d) 60, (e) 80, (f) 100, (g) 120, (h) 140, and (i) 160 pulses.

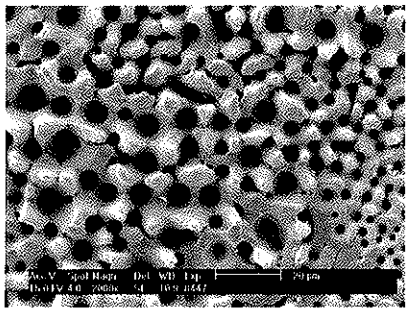

Video 2. File: video 2; Video of SEM images of spike growth on 316 SS with increased pulse count at 2000x magnification. http://dx.doi.org/10.1117/12.2040348.2

4. CONCLUSION

This paper presents the formation process for a specific type of self-organized micro/nanostructure, ASG-mounds, on 316 SS formed using FLSP. ASG-mounds on 316 SS are similar to those formed on Nickel through a similar procedure, but have some differences in their formation process. On 316 SS the precursor sites are in the form of randomly oriented pits. As material is ejected or flows up the walls of each pit the rims form around the pits that eventually collide together.

This collision begins the formation of the ASG-mounds. The difference in formation processes for ASG-mounds on 316 SS versus nickel demonstrates the importance to understanding the formation process for each unique structure on different materials.

ACKNOWLEDGEMENTS

This work has been supported by a Multi-University Research Initiative (MURI) No. – W911NF-06-1-0446, Grant Assistance in Areas of National Need (GAANN) No. – P200A070344, and a grant through the Nebraska Center for Energy Sciences Research (NCESR) with funds provided by Nebraska Public Power District (NPPD) to the University of Nebraska-Lincoln (UNL) No. 4200000844.

REFERENCES

[1] Iyengar, V. V., Nayak, B. K. and Gupta, M. C., "Optical properties of silicon light trapping structures for photovoltaics," Sol. Energ. Mat. Sol. C. 94(12), 2251–2257 (2010).

[2] Nayak, B. K., Gupta, M. C. and Kolasinski, K. W., "Spontaneous formation of nanospiked microstructures in germanium by femtosecond laser irradiation," Nanotechnology 18(19), 195302 (2007).

[3] Bonse, J., Baudach, S., Krüger, J., Kautek, W. and Lenzner, M., "Femtosecond laser ablation of silicon-modification thresholds and morphology," Appl. Phys. A-Mater. 74(1), 19–25 (2002).

[4] Kolasinski, K.W., Mills, D. and Nahidi, M., "Laser assisted and wet chemical etching of silicon nanostructures," J. Vac. Sci. Technol. A. 24(4), 1474 (2006).

[5] Zorba, V., Boukos, N., Zergioti, I. and Fotakis, C., "Ultraviolet femtosecond, picosecond and nanosecond laser microstructuring of silicon: structural and optical properties," Appl. Optics 47(11), 1846–50 (2008).

[6] Zhu, J., Yin, G., Zhao, M., Chen, D. and Zhao, L., "Evolution of silicon surface microstructures by picosecond and femtosecond laser irradiations," Appl. Surf. Sci. 245(1-4), 102–108 (2005).

[7] Zorba, V., Alexandrou, I., Zergioti, I., Manousaki, A., Ducati, C., Neumeister, A., Fotakis, C. and Amaratunga, G. A. J., "Laser microstructuring of Si surfaces for low-threshold field-electron emission," Thin Solid Films 453-454, 492–495 (2004).

[8] Her, T. H., Finlay, R. J., Wu, C. and Mazur, E., "Femtosecond laser-induced formation of spikes on silicon," Appl. Phys. A-Mater. 70, 383–385 (2000).

[9] Tull, B. R., Carey III, J. E., Mazur, E., McDonald, J. P. and Yalisove, S. M., "Silicon surface morphologies after femtosecond laser irradiation," MRS Bull. 31(08), 626–633 (2011).

[10] Crouch, C. H., Carey III, J. E., Warrender, J. M., Aziz, M. J., Mazur, E. and Génin, F.Y., "Comparison of structure and properties of femtosecond and nanosecond laser-structured silicon," Appl. Phys. Lett. 84(11), 1850 (2004).

[11] Zuhlke, C. A., Anderson, T. P. and Alexander, D. R., "Formation of multiscale surface structures on nickel via above surface growth and below surface growth mechanisms using femtosecond laser pulses," Opt. Express 21(7), 8460–73 (2013).

[12] Zuhlke, C. A., Anderson, T. P. and Alexander, D. R., "Fundamentals of layered nanoparticle covered pyramidal structures formed on nickel during femtosecond laser surface interactions," Appl. Surf. Sci. 21(7), 8460–73 (2013).

[13] Zuhlke, C. A., Anderson, T. P. and Alexander, D. R., "Comparison of the structural and chemical composition of two unique micro/nanostructures produced by femtosecond laser interactions on nickel," Appl. Phys. Lett. 103(12), 121603 (2013).

[14] Sánchez, F., Morenza, J. L., Aguiar, R., Delgado, J. C. and Varela, M., "Dynamics of the hydrodynamical growth of columns on silicon exposed to ArF excimer-laser irradiation," Appl. Phys. A-Mater. 66(1), 83–86 (1998).

[15] Sanchez, F., Morenza, J. L. and Trtik, V., "Characterization of the progressive growth of columns by excimer laser irradiation of silicon," Appl. Phys. Lett. 75(21), 3303 (1999).

[16] Wu, B., Zhou, M., Li, J., Ye, X., Li, G. and Cai, L., "Superhydrophobic surfaces fabricated by microstructuring of stainless steel using a femtosecond laser," Appl. Surf. Sci. 256, 61–66 (2009).

[17] Nayak, B. K. and Gupta, M. C., "Self-organized micro/nano structures in metal surfaces by ultrafast laser irradiation," Opt. Laser. Eng. 48, 940–949 (2010).
[18] Semaltianos, N. G., Perrie, W., French, P., Sharp, M., Dearden, G. and Watkins, K. G., "Femtosecond laser surface texturing of a nickel based superalloy," Appl. Surf. Sci. 255, 2796–2802 (2008).
[19] Bizi-Bandoki, P., Benayoun, S., Valette, S., Beaugiraud, B. and Audouard, E., "Modifications of roughness and wettability properties of metals induced by femtosecond laser treatment," Appl. Surf. Sci. 257, 5213–5218 (2011).
[20] Kuršelis, K., Kiyan, R. and Chichkov, B. N., "Formation of corrugated and porous steel surfaces by femtosecond laser irradiation," Appl. Surf. Sci. 258, 8845–8852 (2012).
[21] Semaltianos, N. G., Perrie, W., French, P., Sharp, M., Dearden, G., Logothetidis, S. and Watkins, K. G., "Femtosecond laser ablation characteristics of nickel-based superalloy C263," Appl. Phys. A-Mater. 94, 999–1009 (2008).
[22] Vorobyev, A. Y. and Guo, C., "Femtosecond laser structuring of titanium implants," Appl. Surf. Sci. 253, 7272–7280 (2007).
[23] Tsukamoto, M., Kayahara, T., Nakano, H., Hashida, M., Katto, M., Fujita, M., Tanaka, M. and Abe, N., "Microstructures formation on titanium plate by femtosecond laser ablation," J. Phys. Conf. Ser. 59, 666–669 (2007).
[24] Jia, W., Peng, Z., Wang, Z., Ni, X. and Wang, C., "The effect of femtosecond laser micromachining on the surface characteristics and subsurface microstructure of amorphous FeCuNbSiB alloy," Appl. Surf. Sci. 253, 1299–1303 (2006).
[25] Shen, M. Y., Crouch, C. H., Carey III, J. E., Younkin, R., Mazur, E., Sheehy, M. and Friend, C. M., "Formation of regular arrays of silicon microspikes by femtosecond laser irradiation through a mask," Appl. Phys. Lett. 82, 1715 (2003).
[26] Singh, A. P., Kapoor, A., Tripathi, K. N., and Kumar, G. R., "Laser damage studies of silicon surfaces using ultra-short laser pulses," Opt. Laser Technol. 34, 37–43 (2002).